Loss of α-tubulin polyglutamylation in ROSA22 mice is associated with abnormal targeting of KIF1A and modulated synaptic function

Koji Ikegami*, Robb L. Heier†, Midori Taruishi*‡, Hiroshi Takagi*, Masahiro Mukai*, Shuichi Shimma§, Shu Taira*, Ken Hatanaka*‡¶, Nobuhiro Morone‖, Ikuko Yao*, Patrick K. Campbell†, Shigeki Yuasa‖, Carsten Janke**, Grant R. MacGregor†,††, and Mitsutoshi Setou*‡§‡‡

*Mitsubishi Kagaku Institute of Life Sciences, Machida, Tokyo 194-8511, Japan; ‡PRESTO, Japan Science and Technology Agency, Kawaguchi City, Saitama 332-0012, Japan; §National Institute for Physiological Sciences, Okazaki, Aichi 444-8787, Japan; †Department of Developmental and Cell Biology, Developmental Biology Center, and Center for Molecular and Mitochondrial Medicine and Genetics, University of California, Irvine, CA 92697-3940; ¶Laboratory of Neurobiophysics, School of Pharmaceutical Sciences, University of Tokyo, Tokyo 113-0033, Japan; ‖Department of Ultrastructural Research, National Institute of Neuroscience, National Center of Neurology and Psychiatry, Kodaira, Tokyo 187-8502, Japan; and **Centre de Rechérches en Biochimie Macromoléculaire, Centre National de la Recherche Scientifique, 34293 Montpellier, France

Communicated by Douglas C. Wallace, University of California, Irvine College of Medicine, Irvine, CA, December 27, 2006 (received for review November 16, 2006)

Microtubules function as molecular tracks along which motor proteins transport a variety of cargo to discrete destinations within the cell. The carboxyl termini of α- and β-tubulin can undergo different posttranslational modifications, including polyglutamylation, which is particularly abundant within the mammalian nervous system. Thus, this modification could serve as a molecular ''traffic sign'' for motor proteins in neuronal cells. To investigate whether polyglutamylated α-tubulin could perform this function, we analyzed ROSA22 mice that lack functional PGs1, a subunit of α-tubulin-selective polyglutamylase. In wild-type mice, polyglutamylated α-tubulin is abundant in both axonal and dendritic neurites. ROSA22 mutants display a striking loss of polyglutamylated α-tubulin within neurons, including their neurites, which is associated with decreased binding affinity of certain structural microtubule-associated proteins and motor proteins, including kinesins, to microtubules purified from ROSA22-mutant brain. Of the kinesins examined, KIF1A, a subfamily of kinesin-3, was less abundant in neurites from ROSA22 mutants *in vitro* and *in vivo*, whereas the distribution of KIF3A (kinesin-2) and KIF5 (kinesin-1) appeared unaltered. The density of synaptic vesicles, a cargo of KIF1A, was decreased in synaptic terminals in the CA1 region of hippocampus in ROSA22 mutants. Consistent with this finding, ROSA22 mutants displayed more rapid depletion of synaptic vesicles than wild-type littermates after high-frequency stimulation. These data provide evidence for a role of polyglutamylation of α-tubulin *in vivo*, as a molecular traffic sign for targeting of KIF1 kinesin required for continuous synaptic transmission.

kinesin | microtubules | synaptic vesicles | trafficking | tyrosination

Microtubules have important roles in intracellular transport, cell motility, cell division, and cell morphogenesis. Neuronal cells use this component of the cytoskeleton to distribute a wide variety of cargo to neurite terminals that can be farther than 1 m from the cell body. Molecular motors transport synaptic vesicle precursors (1), neurotransmitter receptors (2, 3), and organelles such as mitochondria (4) along the microtubule network to their appropriate subcellular destinations, i.e., axonal terminals or dendrites (5). A central question in biology is how the molecular motors discriminate among the different microtubules within the cell. One potential mechanism to facilitate molecular heterogeneity of microtubules involves application of a variety of posttranslational modifications (PTMs) to the exposed carboxyl-terminal tails of tubulin (6, 7), such as detyrosination/tyrosination (8, 9), polyglycylation (10, 11), and polyglutamylation (12). Brain tubulin is subject to each of these PTMs. Thus, PTM of discrete subpopulations of microtubules in the cell might serve as molecular "traffic signs" or "directional cues" for different molecular motors.

Enzymes that mediate PTM of tubulin carboxyl-terminal tails include a unique family of proteins possessing a tubulin tyrosine ligase (TTL) domain. The original TTL enzyme performs tyrosination of α-tubulin (13, 14). Although a vital role of TTL in neuronal organization has been discovered (15), a function of tubulin tyrosination as a molecular traffic sign for molecular motors has not been demonstrated (15, 16). Recently related members of the enzyme family called tubulin tyrosine ligase-like (TTLL) proteins were identified (17). Mammals have at least a dozen loci capable of encoding independent TTLL proteins (17, 18). Of these proteins, at least two TTLLs can incorporate glutamate to tubulins. TTLL1 is a catalytic subunit of α-tubulin-preferring polyglutamylase (17), whereas TTLL7 preferentially polyglutamylates β-tubulin (18). There is evidence to suggest that cellular activities, e.g., ciliary and flagellar motility (19), neuronal differentiation (18), and centriole stability (20), involve tubulin polyglutamylation. However, despite identification of the enzymes and analysis of their function *in vitro* (17, 18), an *in vivo* function for tubulin polyglutamylation in mammals, especially in the brain, has remained unclear.

To test whether polyglutamylated α-tubulin could function as a molecular traffic sign for molecular motors, we analyzed ROSA22 mice (21) that lack functional PGs1, a component of α-tubulin-preferring polyglutamylase complex (22). Here we provide evidence for a function of α-tubulin polyglutamylation *in vivo*, to regulate intracellular targeting of KIF1 kinesin motor and its cargo synaptic vesicles in neurons and to modulate continuous synaptic transmission.

Results

Tubulin Modification in ROSA22 Mice. PGs1, the protein encoded by *Gtrgeo22* (21), is a noncatalytic subunit of an enzyme complex with polyglutamylase activity preferential to α-tubulin (22). PGs1 is

Author contributions: K.I., G.R.M., and M.S. designed research; K.I., R.L.H., M.T., H.T., M.M., S.S., S.T., K.H., N.M., I.Y., P.K.C., and S.Y. performed research; C.J. and G.R.M. contributed new reagents/analytic tools; K.I., R.L.H., H.T., M.M., S.S., S.T., P.K.C., G.R.M., and M.S. analyzed data; and K.I., G.R.M., and M.S. wrote the paper.

The authors declare no conflict of interest.

Freely available online through the PNAS open access option.

Abbreviations: AMP-PNP, adenosine 5′-[β,γ-imido]triphosphate; CBB, Coomassie brilliant blue; fEPSP, field excitatory postsynaptic potential; MAP, microtubule-associated protein; PTM, posttranslational modification; SCG, superior cervical ganglion; TTL, tubulin tyrosine ligase; TTLL, tubulin tyrosine ligase-like.

††To whom correspondence may be addressed. E-mail: gmacg@uci.edu.

‡‡To whom correspondence may be addressed. E-mail: setou@nips.ac.jp.

This article contains supporting information online at www.pnas.org/cgi/content/full/0611547104/DC1.

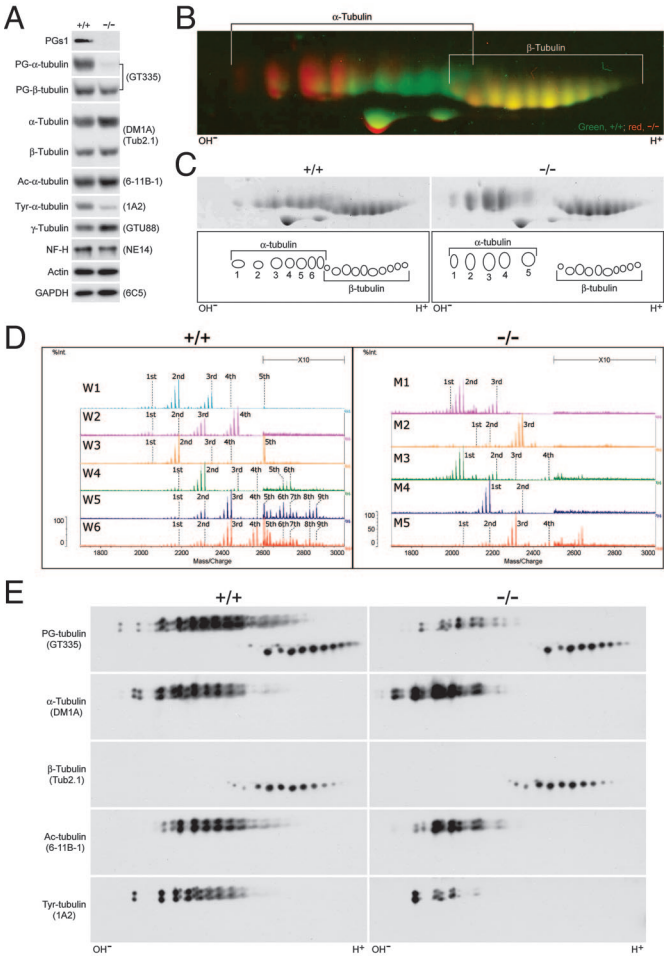

Fig. 1. PTM of tubulin in ROSA22 mutant mice. (*A*) Representative Western blot analysis of tubulins in brain lysates of adult wild-type (+/+) and ROSA22 homozygote (−/−) mice. Brain homogenate of ROSA22 homozygote (−/−) mice lacked PGs1 and contained a significantly less amount of polyglutamylated (PG-) and tyrosinated (Tyr-) tubulin than that of wild-type (+/+) mice. The amounts of acetylated (Ac-), α-, β-, γ-tubulin, neurofilament H (NF-H), actin, and GAPDH were not different between wild-type and ROSA22 homozygote. Quantitative analyses of signal intensities are shown in SI Fig. 9. (*B* and *C*) Brain lysates from wild-type (+/+) and ROSA22 mutant (−/−) were subjected to high-resolution two-dimensional electrophoresis. (*B*) The images of CBB-stained two-dimensional gel were colorized and merged; green, wild-type; red, mutant. (*C*) Major spots were numbered. (*D*) Mass spectrometry of the α-tubulin carboxyl terminus digested from major spots shown in the illustration in *C*. (*Left*) Wild type (W). (*Right*) Mutant (M). The spot number corresponds to the numbering in the illustration (e.g., W1 corresponds to the sample 1 in the wild type). The peak detected in each spot was ordered numerically, and the corresponding peptide mass and the deduced carboxyl-terminal modifications are listed in SI Table 1. Formally, as indicated in the table, the mass spectrometry cannot exclude the existence of relatively low abundance of biglutamylated forms of Δ2 α-tubulin (Δ2 + 2E). (*E*) Western blot analysis of high-resolution two-dimensional electrophoresis of tubulins from brains of wild-type and homozygous ROSA22 mice. The blot was probed in sequence with antibodies against polyglutamylated, α-, β-, acetylated, and tyrosinated tubulin.

expressed in testis and in the nervous system [see supporting information (SI) Fig. 7], where polyglutamylated tubulin is prominent (23). PGs1 functions as a scaffold protein to localize a catalytic subunit of polyglutamylase to tubulin or microtubules (SI Fig. 8). To investigate functions for α-tubulin polyglutamylation *in vivo*, we analyzed ROSA22 mutant mice, which have a mutation in *Gtrgeo22* (21) that results in a loss of native PGs1 (Fig. 1*A*). We first analyzed the status of the PTM of tubulin extracted from brains of ROSA22 mutant mice by Western blotting with GT335 monoclonal antibody (mAb) that recognizes both mono- and polyglutamylated tubulin (23). ROSA22 mutants displayed a dramatic reduction in steady-state level of polyglutamylated α-tubulin (Fig. 1*A* and SI Fig. 9). No difference was observed in the steady-state level of acetylated α-tubulin, whereas tyrosinated α-tubulin was also decreased in ROSA22 mutants (Fig. 1*A* and SI Fig. 9). Analysis by high-resolution two-dimensional PAGE (Fig. 1*B*) verified that only α-tubulin was grossly affected by the loss of PGs1 function in ROSA22 mutants. In ROSA22 mutants, the relatively acidic forms of α-tubulin found in wild-type mice were replaced with new, more basic forms (Fig. 1*B*), suggesting a gross loss of the polyglutamate side chain on α-tubulin in brains of ROSA22 mutants. Consistent with this interpretation, mass spectrometry of major α-tubulin spots in Coomassie brilliant blue (CBB)-stained gel detected only monoglutamylated forms of α-tubulin in brains of ROSA22 mutants (Fig. 1 *C* and *D* and SI Table 1). We verified these findings by two-dimensional PAGE/Western blot analyses, which demonstrated a decrease in the numbers of polyglutamylated and tyrosinated α-tubulin species (Fig. 1*E*). This analysis also revealed an extremely minor reduction of highly polyglutamylated species of β-tubulin. Thus, ROSA22 mice can be used to investigate the physiological function of α-tubulin polyglutamylation as a molecular traffic sign for molecular motors in the nervous system *in vivo*.

Intracellular Distribution of Polyglutamylated Tubulin. If PTM of tubulin regulates targeting of different molecular motors *in vivo*, cells should display discrete subcellular distribution of microtubules with different PTMs. To investigate the subcellular distribution of polyglutamylated α-tubulin in neurons, we cultured explanted superior cervical ganglia (SCG) and dissected them into neurites and cell bodies. Consistent with the prediction, polyglutamylated α-tubulin was enriched in neurites, whereas modified β-tubulin was concentrated in soma (Fig. 2*A*) (18). To investigate further the subcellular distribution of polyglutamylated α-tubulin, we performed immunocytochemical staining of cultured hippocampal neurons with B3 mAb. This antibody has been reported to react with both polyglutamylated α- and β-tubulin derived from mouse brain (19). Surprisingly, under the experimental conditions used, we found that mAb B3 selectively recognized glutamylated α-tubulin (SI Fig. 10). Both axonal and dendritic processes contained polyglutamylated α-tubulin (Fig. 2*B*). *In vivo*, polyglutamylated α-tubulin was localized predominantly in process-rich regions, e.g., the molecular layer of cerebellum (Fig. 2*C*). These findings support a model for a function of polyglutamylated α-tubulin as a molecular traffic sign for targeting of certain motor proteins into these structures.

Effects of α-Tubulin Polyglutamylation on Binding of Motor Proteins to Microtubules. The binding affinity of kinesin motors to microtubules *in vitro* can be affected by the extent of tubulin polyglutamylation (5, 24). To investigate whether α-tubulin polyglutamylation affects binding of kinesins to microtubules, we analyzed the ability of kinesins to copurify with microtubules isolated from brains of ROSA22 mutant and control mice (Fig. 3*A*). Because binding affinities of structural microtubule-associated proteins (MAPs) can also be affected differently by the extent of tubulin polyglutamylation (25, 26), we also investigated the ability of MAPs to be coprecipitated with microtubules. In the presence of ATP, which promotes detachment of kinesin motors from microtubules, all MAPs analyzed except MAP2 exhibited weaker binding affinity to microtubules isolated from ROSA22 mutants (Fig. 3*B*). In the presence of adenosine 5′-[β,γ-imido]triphosphate (AMP-PNP), which inhibits detachment of kinesins from microtubules, KIF1A, KIF5, dynein, and MAP1A displayed weaker binding to microtubules isolated from ROSA22 homozygotes (Fig. 3*B*). No significant difference in total steady-state levels of each MAP and motor protein was observed between wild-type and ROSA22 mutant

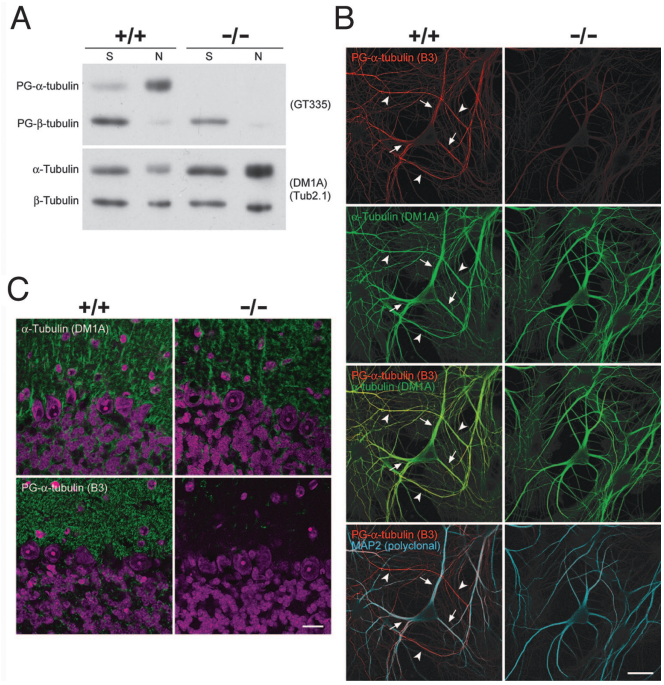

Fig. 2. Intracellular distribution of polyglutamylated tubulins. (*A*) SCG explants from wild-type (+/+) and ROSA22 mutant (−/−) were surgically dissected into soma (S) and neurites (N). To obtain equal amounts of tubulin, soma samples contained 3-fold more protein than samples from neurites. The samples were immunoblotted with antibodies specific for polyglutamylated (PG-) or α- or β-tubulin. (*B*) Hippocampal neuronal cultures from wild-type (+/+) or ROSA22 homozygote mice (−/−) were fixed and stained with mAb B3 that reacted selectively with PG-α-tubulin under the conditions used (SI Fig. 10) together with anti-α-tubulin (mAb, DM1A labeled with FITC) and polyclonal anti-MAP2 antibodies. Both axonal (arrowheads) and dendritic (arrows) processes react with mAb B3. Red, PG-α-tubulin; green, α-tubulin; cyan, MAP2. (Scale bar, 30 μm.) (*C*) Sagittal sections of brain from control (+/+) and ROSA22 mutant (−/−) mice were stained with B3 or DM1A (green) and TOTO-3 (magenta) to identify DNA. (Scale bar, 20 μm.)

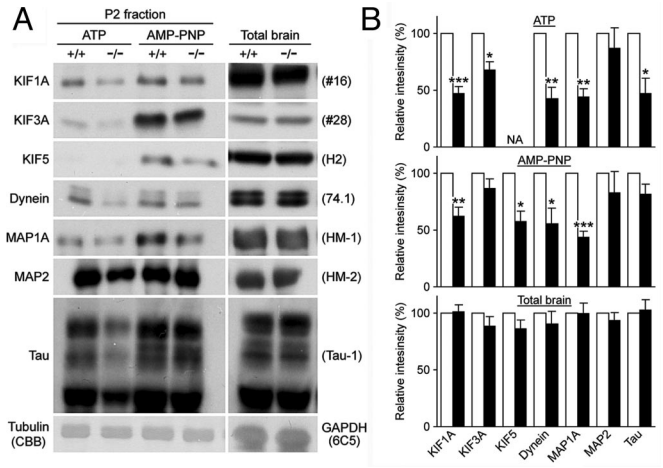

Fig. 3. Effects of α-tubulin polyglutamylation on binding of MAPs to microtubules. (*A*) Crude microtubules were prepared from brain homogenates of wild-type (+/+) or ROSA22 mutant (−/−) in the presence of ATP or AMP-PNP. Cosedimented kinesins and MAPs were detected by Western blot analysis. The amount of protein applied was monitored by the intensity of the CBB-stained tubulin. (*B*) Signal intensities were quantified and are represented as a percentage of mutant signal relative to wild-type signal. (*Top*) ATP-present sample. NA, not applicable. (*Middle*) AMP-PNP-present sample. (*Bottom*) Total brain homogenate (bottom). Open columns, wild type; filled columns, mutant. *, $P < 0.05$; **, $P < 0.01$; ***, $P < 0.001$, with paired *t* test.

brains (Fig. 3*B*). These results indicate that polyglutamylation of α-tubulin influences the *in vitro* binding properties of a broad range of MAPs, but in particular, KIF1A, KIF5, cytosolic dynein, and MAP1A. The results also raise the possibility that binding of those MAPs to microtubules *in vivo* could be altered in neurons in ROSA22 mice.

Abnormal KIF1 Distribution in PGs1-Deficient Neurons and Mice. To investigate the role of α-tubulin polyglutamylation in targeting molecular motors to subcellular destinations, we analyzed the distribution of kinesin motors in SCG explants cultured from wild-type and ROSA22 mutant mice. The distribution of KIF1A was altered in explants of SCG from ROSA22 mutant mice, with KIF1A being reduced in neurites compared with controls (Fig. 4 *A* and *B*). As an independent method to verify this finding, we transfected hippocampal neurons isolated from wild-type and ROSA22 mutant mice with green (GFP) or yellow (YFP) fluorescent protein-tagged KIF1A and KIF5A kinesins (Fig. 4*C*). A GFP-KIF1A fusion protein entered neurites in cultured hippocampal neurons from wild-type but not ROSA22 mutant mice (Fig. 4*C*). In contrast, a YFP-tagged KIF5A entered neurites in cells from animals of both genotypes (Fig. 4*C*). *In vivo*, KIF1A was present in regions enriched by polyglutamylated α-tubulin, e.g., the molecular layer of cerebellum (Figs. 2*C* and 4*D*). In ROSA22 mutants, immunoreactivity for KIF1A was greatly reduced in this structure (Fig. 4*D*). The difference in the extent of reduction of KIF1A in the molecular layer of the cerebellum compared with neurites of explanted SCG could be the result of several factors, including the different cell types (*in vitro* versus *in vivo*) and analytical methods (Western blotting versus immunofluorescence). However, in each case, the steady-state level of KIF1A is clearly reduced in neuronal processes. Taken together, these results demonstrate that in at least some populations of neurons, targeting of KIF1A into neurites is influenced by α-tubulin polyglutamylation.

Mislocalization of KIF1A Cargo, Synaptic Vesicles, in PGs1-Deficient Mice. Impaired targeting of KIF1A into neuronal processes in brains of ROSA22 mutant mice should be associated with altered distribution of KIF1A-dependent cargo, such as synaptic vesicles (1). Indeed we observed a modest but significant decrease in density of synaptic vesicles in the synaptic terminals of the hippocampal CA1 region in ROSA22 mutant mice compared with wild-type mice (Fig. 5 *A* and *B* and SI Fig. 11). We also analyzed the steady-state level of synaptic vesicle proteins in brains of wild-type and ROSA22 mutant mice. Western blot analysis indicated no significant difference in levels of either synaptotagmin or synaptophysin (SI Fig. 12 *A* and *B*). In addition, N-cadherin, a cargo of KIF3A-containing kinesin-2 motor (27), and amyloid precursor protein, a cargo of KIF5-containing kinesin-1 motor (28), were each distributed similarly in brains of wild-type and ROSA22 mutant mice (SI Fig. 12*C*). Finally, another cargo of kinesin-1, mitochondria (4), was also distributed in a similar manner in neurites in neurons from wild-type and ROSA22 mutant mice (SI Fig. 12*D*). These results are consistent with the selective impairment of KIF1A intracellular distribution in ROSA22 mutant mice.

Impaired Synaptic Transmission in PGs1-Deficient Mice. Given the reduced density of synaptic vesicles observed in ROSA22 mutant mice, we examined whether KIF1A-dependent electrophysiological characteristics are affected in the brains of these animals. Consistent with our findings, a field excitatory postsynaptic potential (fEPSP) induced by a brief high-frequency stimulation (100 Hz, 19 stimuli) within CA3–CA1 synapse was more rapidly attenuated in ROSA22 mutant animals compared with control littermates (Fig. 6*A*). The fEPSP slopes declined faster in brain slices from ROSA22

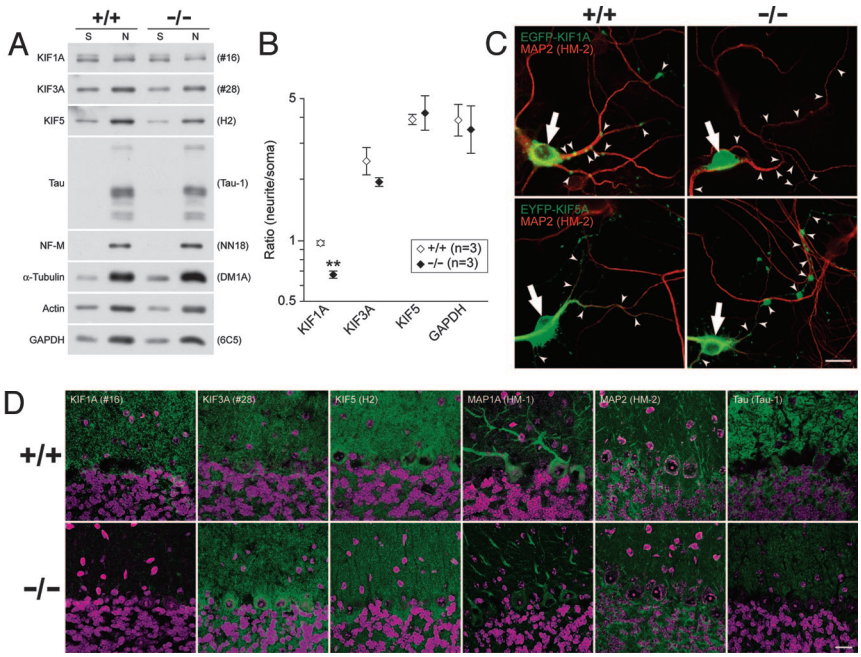

Fig. 4. Altered distribution of KIF1 in ROSA22 mutant neurons and mice. (*A*) Equal amounts of soma (S) and neurite (N) lysates prepared from wild-type (+/+) and ROSA22 mutant (−/−) mice were subjected to Western blot analyses, with antibodies against proteins indicated. (*B*) Signal intensities of bands of KIF1A, 3A, 5, and GAPDH were quantified, and the data are presented as the ratio of the amount in neurites to that in soma. The values presented are mean ± SEM of three independent experiments. **, $P < 0.01$ with paired *t* test. (*C*) In wild-type (+/+) neurons, EGFP-KIF1A is localized in the soma (white arrow) and entered neurites (small white arrowheads). In neurons from ROSA22 homozygotes (−/−), EGFP-KIF1A was present in the soma (white arrow) but was absent from neurites (white arrowheads). In contrast, EYFP-KIF5A (white arrowheads) was able to enter neurites in neurons from both wild-type and ROSA22 homozygous mice. Green, kinesins; red, MAP2. (Scale bar, 20 μm.) (*D*) Sagittal brain sections of control (+/+) and ROSA22 mutant (−/−) mice were stained with antibodies that recognize the proteins indicated (green) and TOTO-3 (magenta). Note that the distribution of Tau and MAP1A appears to be altered in the ROSA22 mutant cerebellum. (Scale bar, 20 μm.)

mutants than in slices from wild-type controls (Fig. 6*B*), and the fEPSP slopes halved significantly faster in ROSA22 homozygote CA3–CA1 synapses (Fig. 6*C*). These data suggest that the docked synaptic vesicles at the active zone are decreased in ROSA22 mice as predicted from the result of EM analysis. In contrast, no difference was observed in the ratio of paired-pulse facilitation, a presynaptic form of short-term synaptic plasticity, between wild-type and ROSA22 homozygotes (Fig. 6*D*), suggesting that the molecular machinery of transmitter release is not impaired. Together, these results support a model where α-tubulin polyglutamylation influences targeting of KIF1A into neurites that alters the amount of docked synaptic vesicles in presynaptic sites, which in turn modulates continuous synaptic transmission.

Discussion

We provide evidence for a role of posttranslational modification (PTM) of α-tubulin in regulating targeting of KIF1 kinesin into neurites. The absence of functional PGs1 in ROSA22 mice results in a dramatic reduction in poly-, but interestingly not monoglutamylated, α-tubulin within the mouse brain. In mouse brain, α-tubulin is polyglutamylated on Glu^{445} (29). Polyglutamylation of

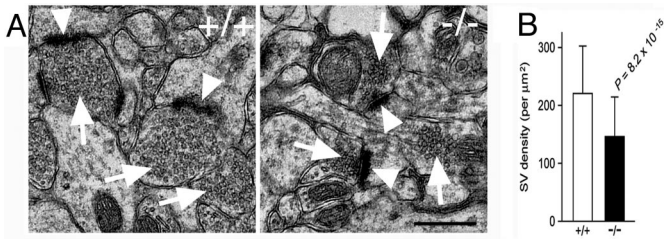

Fig. 5. Mislocalization of synaptic vesicles, cargoes of KIF1A, in ROSA22 mutant mice. (*A*) Representative example of ultrastructure of the CA1 region of hippocampus in wild-type (+/+) and ROSA22 mutant (−/−) mice. Synaptic vesicles (arrowheads) and the postsynaptic side of the synaptic density (arrow) are indicated. (Scale bar, 500 nm.) (*B*) The density of synaptic vesicles in synaptic terminals was quantified from three independent mice of each genotype.

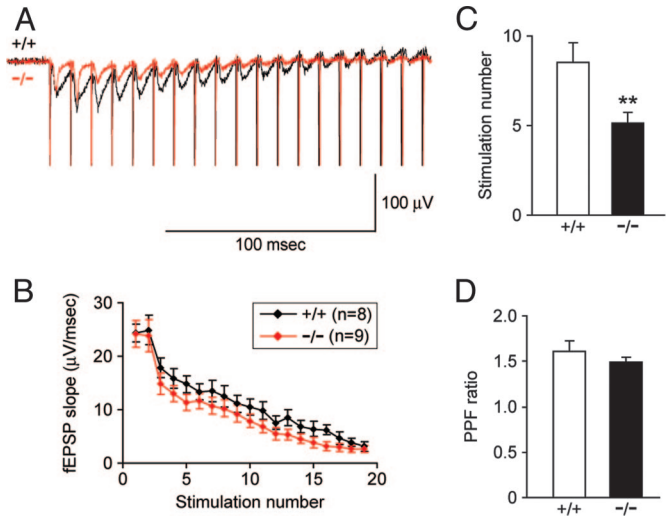

Fig. 6. Impaired synaptic transmission in ROSA22 mutant mice. (*A*) Hippocampal slices were subjected to a brief high-frequency stimulation (100 Hz, 19 pulses). The fEPSP slopes during the entire high-frequency stimulation were recorded from CA1 synapses of wild-type (+/+, black) and ROSA22 mutant (−/−, red) mice. (*B*) Plot of fEPSP slope against stimulus no. (*C*) Stimulation no. where fEPSP slopes halved are shown. The data represented are mean ± SEM ($n = 8$ for wild-type, +/+; $n = 9$ for mutant, −/−). **, $P < 0.01$ with Student's *t* test. (*D*) Paired-pulse facilitation (PPF) was quantified by using the ratios of the second to the first fEPSP slopes at interpulse intervals of 50 ms.

tubulin presumably first requires ligation of glutamate through its amide group to the γ-carboxyl side chain of Glu^{445} to generate monoglutamylated α-tubulin. Subsequently, additional glutamates are added in a conventional manner through the α-carboxyl group of the monoglutamate to generate bi-, tri-, etc. polyglutamylated α-tubulin (29). Analysis of ROSA22 mutant mice indicates that these activities are distinct; i.e., the polyglutamylase activity is PGs1-dependent, whereas the monoglutamylase activity is PGs1-independent. Thus, at least two discrete enzymatic activities are capable of adding glutamate to α-tubulin in the mouse brain.

As reported recently (18), the discrete distribution of polyglutamylated α-tubulin in neuronal cells is striking. Polyglutamylated α-tubulin appears to have a similar distribution within axons and dendrites, which suggests that α-tubulin polyglutamylation by itself is unlikely to function as a molecular signpost to facilitate discrimination between axonal and dendritic microtubules. One possibility is that this modification could function as part of a combinatorial code of tubulin modification that allows molecular machinery to discriminate between these subcellular compartments. In hippocampal neurons in culture, KIF1 is distributed evenly in both axonal and dendritic processes (30), whereas KIF5 displays a highly polarized, i.e., axon-preferential distribution (30, 31). Our results indicate that α-tubulin polyglutamylation positively influences movement of a "nonpolar kinesin" KIF1 from soma into neurites. However, this specific modification appears to have no direct influence on the axon-selective distribution of a "polar kinesin" KIF5. Polarized targeting of kinesins such as KIF5 might be regulated by other tubulin modifications, such as β-tubulin polyglutamylation or monoglutamylation of either α- or β-tubulin.

A model can be proposed for a molecular mechanism as to why the distribution of KIF1 is affected by loss of α-tubulin polyglutamylation whereas distributions of KIF3 and KIF5 appear unaffected. The model is based on a unique molecular characteristic of KIF1. KIF1 moves along microtubules by "biased Brownian movement" (32) because it can function as a monomeric motor (4). KIF1 is attracted to the negatively charged α-tubulin carboxyl terminus while transiting a weak-binding state during biased Brownian movement (33, 34). The long positively charged K loop present in KIF1 (32) can interact strongly with the highly negatively charged polyglutamate side chain on α-tubulin (33). This ionic force may be required to maintain interaction between monomeric forms of KIF1A and microtubules *in vivo*. Thus, loss of α-tubulin polyglutamylation in ROSA22 mutants would impair KIF1–microtubule interaction, when KIF1 is in the weak-binding state. In contrast, KIF5–microtubule binding is mediated mainly by interaction between the short K loop of KIF5 and the C terminus of β-tubulin (35, 36). Unlike KIF1, KIF5 invariably functions as a dimer and has two motor heads, which allows it to maintain attachment to microtubules by one motor head while the other head glides over the tubulin surface. Consequently, movement of kinesins other than KIF1 may be relatively insensitive to the loss of α-tubulin polyglutamylation. Under this model, other tubulin modifications, such as β-tubulin polyglutamylation, α- and β-tubulin monoglutamylation, and tubulin acetylation, or combinations of such modifications, may affect the trafficking of other kinesins. This model is consistent with a recent report that acetylation of α-tubulin, despite being located on the inner lumen of microtubules, affects binding and transport of kinesin-1 (37).

Our model predicts that changes in polyglutamylation of α-tubulin are the underlying cause of altered distribution of KIF1 and modulated synaptic function in ROSA22 mice. However, it is important to consider whether other mechanisms could be responsible for these effects. ROSA22 mutant mice also displayed a decrease in tyrosinated α-tubulin. At present, the mechanism underlying this additional change is unclear. During differentiation of mouse neurons in culture, polyglutamylation and detyrosination [to produce Δ2-tubulin (38)] of α-tubulin display similar kinetics (39), which raises the possibility that these posttranslational changes may be coordinated, as has been observed for other PTMs of tubulin (11). In the case of ROSA22 mutant mice, the reduction in tyrosinated tubulin might be a consequence of the imbalance in α-tubulin polyglutamylation.

Could a reduction in tyrosinated α-tubulin be responsible for altered distribution of kinesins in ROSA22 mice? Conventional kinesin can bind with greater affinity to detyrosinated tubulin than to tyrosinated tubulin (40, 41). Given the reduced level of tyrosinated tubulin in ROSA22 mutant mice, kinesins might be expected to bind more strongly to ROSA22 mutant-derived microtubules. However, our results indicate that kinesins, including conventional (KIF5) and monomeric (KIF1) kinesins, actually displayed weaker binding affinity to ROSA22 mutant-derived microtubules than to wild-type-derived microtubules. Although we cannot currently exclude the possibility that the reduced level of tyrosinated tubulin (or, the increased level of detyrosinated tubulin) contributes to mislocalization of KIF1 and the defect of synaptic transmission we observed in ROSA22 mutants, a mechanism for such an effect is not immediately apparent. Lastly, it is also formally possible that loss of function of PGs1 affects localization of KIF1 in a mechanism independent of the status of PTM of tubulin.

The loss of polyglutamylated α-tubulin was associated with more rapid attenuation of synaptic transmission. It is of interest that loss of polyglutamylation of α-tubulin produces a relatively subtle mutant phenotype in mice. Our results indicate that the level of KIF1A is reduced, but not absent, in at least a subset of neurites in ROSA22 mutant mice. A more processive form of dimeric Unc104/KIF1A (42) can successfully enter neurites as can KIF5. Thus, residual monoglutamylated α-tubulin may facilitate targeting of KIF1 into neurites with reduced efficiency. Alternatively, this process might occur in an α-tubulin polyglutamylation-independent manner. Finally, β-tubulin polyglutamylation may be able to compensate in part for loss of polyglutamylated α-tubulin. The persistence of reduced levels of KIF1A within some neurites would explain why ROSA22 homozygotes do not display a lethal phenotype as found in KIF1A-deficient mice (43).

In conclusion, based on our findings we propose a model where PTM of tubulin modulates synaptic transmission through proper targeting of a kinesin motor to its destination. An interesting question concerns whether alterations in the steady-state level of PTM of tubulin might either be associated with, or contribute to, development of common neuronal pathologies associated with altered binding of MAPs or synaptic function such as schizophrenia or Alzheimer's disease.

Materials and Methods

Mice. ROSA22 mutant mice were generated as described previously (21). All experimentation with mice was conducted under protocols approved by Institutional Animal Care and Use Committees of the respective institutions.

Antibodies and Western Blot Analysis. Anti-PGs1 polyclonal antibody was raised in rabbits by using maltose-binding protein-fused PGs1 as a substrate. Recombinant PGs1 was purified by amylose resin (New England Biolabs, Ipswich, MA), mixed with Freund's adjuvant (Sigma–Aldrich, St. Louis, MO) and injected s.c. on the dorsum of rabbits. Specificity of the antibody was confirmed by Western blot analysis comparing protein from wild-type and ROSA22 mutant mice. GT335 mAb, which reacts with both glutamylated forms of α- and β-tubulin (23), was a kind gift from B. Eddé (CNRS, Montpellier, France). B3 mAb, which is reported to have specificity for poly (bi+)- glutamylated tubulins (19), was purchased from Sigma–Aldrich (catalog no. T9822). For an unknown reason, under the experimental conditions used, the specific lot (no. 022K4805) used in these studies reacted with glutamylated α-tubulin but not glutamylated β-tubulin (SI Fig. 10). Information on all other antibodies used and the method of Western blotting is provided in *SI Materials and Methods*.

Two-Dimensional Electrophoresis. Tissues were homogenized in lysis buffer (7 M urea/2 M thiourea/2% CHAPS/40 mM DTT/2% IPG buffer, pH 3–10), and samples were subjected to isoelectric focusing (IEF) in an immobilized pH linear gradient gel (IPG gel) of pH 4.5–5.5, 24 cm in length (Amersham, Piscataway, NJ). Second-dimensional gel electrophoresis was performed by using laboratory-cast SDS/polyacrylamide gels (12%). A detailed protocol for IEF is provided in *SI Materials and Methods*.

Mass Spectrometry. Protein spots in gel were excised, rinsed in acetonitrile, dehydrated, and reduced. After alkylation, the samples were incubated overnight at 37°C in digestion buffer containing endopeptidase Lys-C. Peptides were extracted and applied to a MALDI plate, and 2,5-dihydroxybenzoic acid was applied to the peptide to form cocrystals. Mass spectrometry was performed as described (44, 45). A detailed protocol is available in *SI Materials and Methods*.

Primary Culture. Hippocampal culture was prepared as described previously (46) with the modifications listed in *SI Materials and Methods*. Microexplants of mouse superior cervical ganglion were prepared as described previously (47) and cultured on a poly-L-lysine- and laminin-coated plastic dish.

Immunocytochemistry, Immunohistochemistry, and Electron Microscopy. These anatomical and morphological analyses were performed by using modifications of standard methods. For detailed information on specific methods, see *SI Materials and Methods*. To determine the density of synaptic vesicles, 10 fields of view that each contained at least 32 nerve terminals with postsynaptic density were photographed randomly, and the numbers of synaptic vesicles in each nerve terminal were counted. Three independent mice were analyzed for each strain. Data represent mean ± SD ($n = 151$ for wild type, $n = 136$ for mutant). Statistical analysis was done with one-way ANOVA.

Cosedimentation Assay of MAPs. Crude tubulin was prepared from an adult mouse brain by one cycle of assembly-disassembly in PIPES buffer (100 mM PIPES, pH 6.8/1 mM EGTA/1 mM $MgSO_4$) containing a mixture of protease inhibitors (10 μM PMSF/10 μg/ml leupeptin). The brains were homogenized in the buffer and centrifuged at 4°C (50,000 × *g* for 30 min). Either 1 mM ATP (pH 6.8) or 1 mM AMP-PNP (pH 6.8) was added to the supernatant containing 1 mM GTP and 20% glycerol. The supernatant was then incubated at 37°C for 35 min. After the incubation, 20 μM Taxol was added to the mixture. After centrifugation at 150,000 × *g* for 40 min at 37°C, the pellet was boiled in SDS/PAGE sample buffer. The amounts of tubulin in samples were determined by electrophoresis of the samples and staining of tubulins with CBB. Data represent mean ± SEM from five independent experiments. Statistical analysis was performed by using a paired *t* test.

Electrophysiology. Hippocampal slices were prepared essentially as described (48) with modifications shown in *SI Materials and Methods*.

We thank an anonymous reviewer for extremely helpful comments; Dr. B. Eddé for mAb GT335 and constructive discussions; members of the Mitsubishi Kagaku Institute of Life Sciences, especially Mr. Nakamura, Ms. Ichinose, Ms. Hinohara, and Dr. Omori, and other members of the M.S. laboratory, especially Ms. Yasutake, Ms. Miyaike, and Ms. Takamatsu, for technical assistance and advice; Drs. Nagai and Sekiya, and Prof. Hirokawa for generous support and constructive discussion. This research was supported by Japan Society for the Promotion of Science (JSPS) WAKATE-B Grant 17700327 (to K.I.), Ministry of Health, Labor, and Welfare Grant NANO-001 (to N.M.), National Institute of Biomedical Innovation Grant 05-32 (to S.Y.), Fondation pour la Recherche Médicale Award INE20021108027/1, and a European Molecular Biology Organization Fellowship ALTF 387-2001 (to C.J.); a grant from the National Institute of Child Health and Human Development/National Institutes of Health (to G.R.M.); and Japan Science and Technology Agency PRESTO and SENTAN grants and JSPS WAKATE-A Grant 17680037 (to M.S.).

1. Okada Y, Yamazaki H, Sekine-Aizawa Y, Hirokawa N (1995) *Cell* 81:769–780.
2. Setou M, Nakagawa T, Seog DH, Hirokawa N (2000) *Science* 288:1796–1802.
3. Setou M, Seog DH, Tanaka Y, Kanai Y, Takei Y, Kawagishi M, Hirokawa N (2002) *Nature* 417:83–87.
4. Tanaka Y, Kanai Y, Okada Y, Nonaka S, Takeda S, Harada A, Hirokawa N (1998) *Cell* 93:1147–1158.
5. Setou M, Hayasaka T, Yao I (2004) *J Neurobiol* 58:201–206.
6. Rosenbaum J (2000) *Curr Biol* 10:R801–R803.
7. Westermann S, Weber K (2003) *Nat Rev Mol Cell Biol* 4:938–947.
8. Argarana CE, Barra HS, Caputto R (1978) *Mol Cell Biochem* 19:17–21.
9. Gundersen GG, Kalnoski MH, Bulinski JC (1984) *Cell* 38:779–789.
10. Redeker V, Levilliers N, Schmitter JM, Le Caer JP, Rossier J, Adoutte A, Bre MH (1994) *Science* 266:1688–1691.
11. Banerjee A (2002) *J Biol Chem* 277:46140–46144.
12. Eddé B, Rossier J, Le Caer JP, Desbruyères E, Gros F, Denoulet P (1990) *Science* 247:83–85.
13. Barra HS, Arce CA, Argarana CE (1998) *Mol NeuroBiol* 2:133–153.
14. Ersfeld K, Wehland J, Plessmann U, Dodemont H, Gerke V, Weber K (1993) *J Cell Biol* 120:725–732.
15. Erck C, Peris L, Andrieux A, Meissirel C, Gruber AD, Vernet M, Schweitzer A, Saoudi Y, Pointu H, Bosc C, *et al.* (2005) *Proc Natl Acad Sci USA* 102:7853–7858.
16. Peris L, Thery M, Faure J, Saoudi Y, Lafanechere L, Chilton JK, Gordon-Weeks P, Galjart N, Bornens M, Wordeman L, *et al.* (2006) *J Cell Biol* 174:839–849.
17. Janke C, Rogowski K, Wloga D, Regnard C, Kajava AV, Strub JM, Temurak N, van Dijk J, Boucher D, van Dorsselaer A, *et al.* (2005) *Science* 308:1758–1762.
18. Ikegami K, Mukai M, Tsuchida JI, Heier RL, MacGregor GR, Setou M (2006) *J Biol Chem* 281:30707–30716.
19. Gagnon C, White D, Cosson J, Huitorel P, Eddé B, Desbruyères E, Paturle-Lafanechère L, Multigner L, Job D, Cibert C (1996) *J Cell Sci* 109:1545–1553.
20. Bobinnec Y, Khodjakov A, Mir LM, Rieder CL, Edde B, Bornens M (1998) *J Cell Biol* 143:1575–1589.
21. Campbell PK, Waymire KG, Heier RL, Sharer C, Day DE, Reimann H, Jaje JM, Friedrich GA, Burmeister M, Bartness TJ, *et al.* (2002) *Genetics* 162:307–320.
22. Regnard C, Fesquet D, Janke C, Boucher D, Desbruyères E, Koulakoff A, Insina C, Travo P, Eddé B (2003) *J Cell Sci* 116:4181–4190.
23. Wolff A, de Néchaud B, Chillet D, Mazarguil H, Desbruyères E, Audebert S, Eddé B, Gros F, Denoulet P (1992) *Eur J Cell Biol* 59:425–432.
24. Larcher JC, Boucher D, Lazereg S, Gros F, Denoulet P (1996) *J Biol Chem* 271:22117–22124.
25. Boucher D, Larcher JC, Gros F, Denoulet P (1994) *Biochemistry* 33:12471–12477.
26. Bonnet C, Boucher D, Lazereg S, Pedrotti B, Islam K, Denoulet P, Larcher JC (2001) *J Biol Chem* 275:12839–12848.
27. Teng J, Rai T, Tanaka Y, Takei Y, Nakata T, Hirasawa M, Kulkarni AB, Hirokawa N (2005) *Nat Cell Biol* 7:474–482.
28. Kamal A, Stokin GB, Yang Z, Xia CH, Goldstein LS (2000) *Neuron* 28:449–459.
29. Redeker V, Le Caer JP, Rossier J, Prome JC (1991) *J Biol Chem* 266:23461–23466.
30. Jacobson C, Schnapp B, Banker GA (2006) *Neuron* 49:797–804.
31. Nakata T, Hirokawa N (2003) *J Cell Biol* 162:1045–1055.
32. Okada Y, Hirokawa N (1999) *Science* 283:1152–1157.
33. Okada Y, Hirokawa N (2000) *Proc Natl Acad Sci USA* 97:640–645.
34. Okada Y, Higuchi H, Hirokawa N (2003) *Nature* 423:574–577.
35. Hoenger A, Thormählen M, Diaz-Avalos R, Doerhoefer M, Goldie KN, Müller J, Mandelkow E (2000) *J Mol Biol* 297:1087–1103.
36. Skiniotis G, Cochran JC, Müller J, Mandelkow E, Gilbert SP, Hoenger A (2004) *EMBO J* 23:989–999.
37. Reed NA, Cai D, Blasius TL, Jih GT, Meyhofer E, Gaertig J, Verhey KJ (2006) *Curr Biol* 16:2166–2172.
38. Paturle-Lafanechere L, Edde B, Denoulet P, Van Dorsselaer A, Mazarguil H, Le Caer JP, Wehland J, Job D (1991) *Biochemistry* 30:10523–10528.
39. Audebert S, Koulakoff A, Berwald-Netter Y, Gros F, Denoulet P, Edde B (1989) *J Cell Sci* 107:2313–2322.
40. Liao G, Gundersen GG (1998) *J Biol Chem* 273:9797–9803.
41. Kreitzer G, Liao G, Gundersen GG (1999) *Mol Biol Cell* 10:1105–1118.
42. Tomishige M, Klopfenstein DR, Vale RD (2002) *Science* 297:2263–2267.
43. Yonekawa Y, Harada A, Okada Y, Funakoshi T, Kanai Y, Takei Y, Terada S, Noda T, Hirokawa N (1998) *J Cell Biol* 141:431–441.
44. Sugiura Y, Shimma S, Setou M (2006) *Anal Chem* 78:8227–8235.
45. Shimma S, Furuta M, Ichimura K, Yoshida Y, Setou M (2006) *J Mass Spectrom Soc Jpn* 54:133–140.
46. Inoue E, Mochida S, Takagi H, Higa S, Deguchi-Tawarada M, Takao-Rikitsu E, Inoue M, Yao I, Takeuchi K, Kitajima I, *et al.* (2006) *Neuron* 50:261–275.
47. Ikegami K, Koike T (2003) *Neuroscience* 122:617–626.
48. Hatanaka K, Ikegami K, Takagi H, Setou M (2006) *Biochem Biophys Res Commun* 350:610–615.